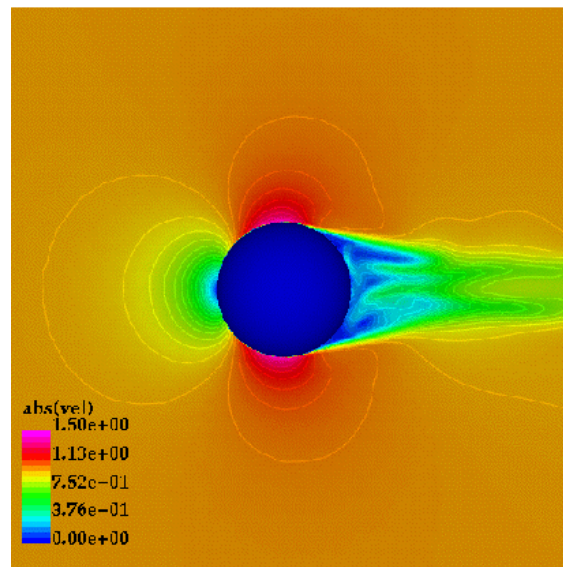




American Institute of
Aeronautics and Astronautics
AIAA-2002-0426

Combining the Baldwin Lomax and Smagorinsky Turbulence Models to Calculate Flows with Separation Regions

F.E. Camelli and R. Löhner
George Mason University, Fairfax, Virginia



40th AIAA Aerospace Sciences
Meeting & Exhibit
14-17 January 2002 / Reno, NV

Combining the Baldwin Lomax and Smagorinsky Turbulence Models to Calculate Flows with Separation Regions

F. Camelli and R.Löhner
School of Computational Sciences
Laboratory for Computational Fluid Dynamics
George Mason University, M.S. 4C7
Fairfax, VA 22030

Abstract

The present paper proposes a combination of the Baldwin Lomax and Smagorinsky turbulence models in order to compensate the deficiencies each one of these simple models exhibits. The proposed combination, named BLS, uses the turbulent viscosity of the Baldwin Lomax in the vicinity of walls, and a blend of Baldwin Lomax and Smagorinsky viscosity from the end of the inner layer (Baldwin Lomax) into the core flow region. Results obtained for a sphere, a cylinder and a cube indicate that the proposed model yields acceptable results, and represents an attractive alternative when transient simulations with wall effects can not be performed with either RANS or LES.

Introduction

Over the last half century, a wide range of turbulence models has been developed to solve the closure problem of the Reynolds Averaged Navier-Stokes equations (RANS). However, it is difficult to find an individual model that can be used reliably over the complete range of turbulent flow cases. These models can be classified according to their complexity as:

algebraic models or *zero equation models* (i.e. based on Prandtl's mixing length hypothesis)

one equation models, *two equation models* (i.e. based on the equation for the turbulence kinetic energy) and

Reynolds-stress models.

An extensive review of these models has been made by Wilcox [1, 2]. Another approach to solve the Navier-Stokes equations is via so-called Large Eddy Simulation

(LES), which assumes that once the inertial scales of the flow have been captured by a sufficiently fine grid, the even shorter (sub-grid) wavelengths can be modeled. This inherently transient approach has been reviewed in detail by Mason [3].

RANS are obtained using a time averaging process, and hence, in principle, are only suitable for stationary problems. However, RANS can be extended to transient problems if the period of the mean (stationary) solution is several orders of magnitude larger than the turbulent fluctuations of the flow. If this condition is not met, RANS cannot be applied for transient problems (a typical example being atmospheric flows).

LES, on the other hand, is a space averaging process and therefore applicable to transient flows for resolving part of the turbulent scales. The limitation is due to the grid size: scales smaller than the grid-size have to be modeled. Many variations exist on closure models for the unresolved scales, from variations of the classic Smagorinsky $h^2 S_2$ [4, 5] to Monotonically Integrated LES (MILES)

© Copyright by the authors. Published by the AIAA with permission.

[6, 7].

The third possibility, solving the Navier-Stokes equations via Direct Numerical Simulation (DNS) [8], resolves all the turbulent scales present in the flow. Due to hardware limitations, this approach can presently only be used in cases with simple geometries/low Reynolds numbers, and does not constitute a feasible option for engineering problems.

Given that RANS and LES are simplified or derived forms of the Navier-Stokes equations, they will have inherent limitations. For example, a wall-bounded flow is extremely difficult to simulate with LES. All the LES variations do not properly resolve the turbulent scales near the wall. A whole branch of research is dedicated to study boundary conditions near the wall. Alternatives to solve this problem are different law-of-the-wall formulations applied as boundary conditions [9, 10]. Flows with regions of separation are difficult to simulate with RANS (algebraic, one- or two-equation models), and their predictions do not always match with experimental data. A relatively new and promising approach is Detached Eddy Simulation (DES). DES merges the best of RANS and LES. RANS is used near the wall where there is no separation. LES is used in the core flow where it works well [11, 12].

This paper approaches the turbulent problem from the point of view of DES. The two simplest algebraic models: Baldwin Lomax [13] and Smagorinsky [4], are combined in such a way that each one is used in the region of the flow it was devised for. The Baldwin Lomax turbulence model is used close to walls, where it is known to give very good results. Smagorinsky is used for regions of separation and core flow. The modified model is then applied to flow past a sphere, a cylinder and a cube in a channel at high Reynolds numbers ($Re = 10^5 - 10^6$).

Turbulence Closures

The turbulence closure model is a term coming from the averaged Navier-Stokes equations for incompressible flows [14]. The resulting term is called Reynolds-stress tensor and it is given by

$$\tau_{ij} = -\overline{u'_j u'_i} \quad (1)$$

where u'_j represents the fluctuating component of u and the over-bar represents the temporal average.

Baldwin Lomax Model

The turbulent eddy viscosity ν_{tur} is calculated in two different ways for the Baldwin Lomax model. There is a distinction between an *inner layer* and an *outer layer*. In the inner layer the viscosity (ν_{tur_i}) is calculated using Equation (2), where the mixing length l_{mix} is given by the Van Driest equation (3). The viscosity in the outer layer (ν_{tur_o}) is calculated with Equation (4).

Inner Layer:

$$\nu_{tur_i} = l_{mix}^2 |\omega|, \quad (2)$$

$$l_{mix} = \kappa y \left[1 - e^{-y^+ / A_0^+} \right], \quad (3)$$

Outer Layer:

$$\nu_{tur_o} = \alpha C_{cp} F_{wake} F_{Kleb}(y; y_{max} / C_{Kleb}), \quad (4)$$

$$F_{wake} = \min [y_{max} F_{max}; C_{wk} y_{max} U_{dif}^2 / F_{max}], \quad (5)$$

$$F_{max} = \frac{1}{\kappa} [\max(l_{mix} |\omega|)]. \quad (6)$$

The constants typically used are:

$$\kappa = 0.40, \quad \alpha = 0.0168, \quad A_0^+ = 26, \quad (7)$$

$$C_{cp} = 1.6, \quad C_{Kleb} = 0.3, \quad C_{wk} = 1.$$

The function F_{Kleb} is Klebanoff's intermittency function given by:

$$F_{Kleb}(y, \delta) = \left[1 + 5.5 \left(\frac{y}{\delta} \right)^6 \right]^{-1}. \quad (8)$$

The magnitude ω is the module of the vorticity vector and U_{dif} is the maximum value of U for boundary layers given in Equation (9).

$$U_{dif} = \left(\sqrt{U^2 + V^2 + W^2} \right)_{max} - \left(\sqrt{U^2 + V^2 + W^2} \right)_{min}. \quad (9)$$

Smagorinsky Model

The Reynolds-stress tensor (Equation 1) is modeled by Equation (10) in the Smagorinsky closure.

$$\tau_{ij} = 2\nu_{tur}S_{ij}, \quad (10)$$

$$S_{ij} = \frac{1}{2} \left(\frac{\partial U_i}{\partial x_j} + \frac{\partial U_j}{\partial x_i} \right). \quad (11)$$

where S_{ij} is the resolved strain rate and ν_{tur} is the Smagorinsky eddy viscosity given by

$$\nu_{tur} = (C_s h)^2 \sqrt{S_{ij}S_{ij}}. \quad (12)$$

where h is the grid scale and C_s is the Smagorinsky coefficient, the value of which lies in the range $0.10 < C_s < 0.24$.

Baldwin-Lomax-Smagorinsky (BLS) Model

The new hybrid turbulence closure, named BLS, consists of a blend of Baldwin Lomax and Smagorinsky models. It is known that Baldwin Lomax has good agreement with the experiments for attached flows or near walls. LES, on the other hand, gives best results in the core flow. The idea is to use each model where it performs best. The algorithm to calculate the viscosity with this new closure is depicted in Figure 1. The functional form of both models is similar and this makes it easy to blend them.

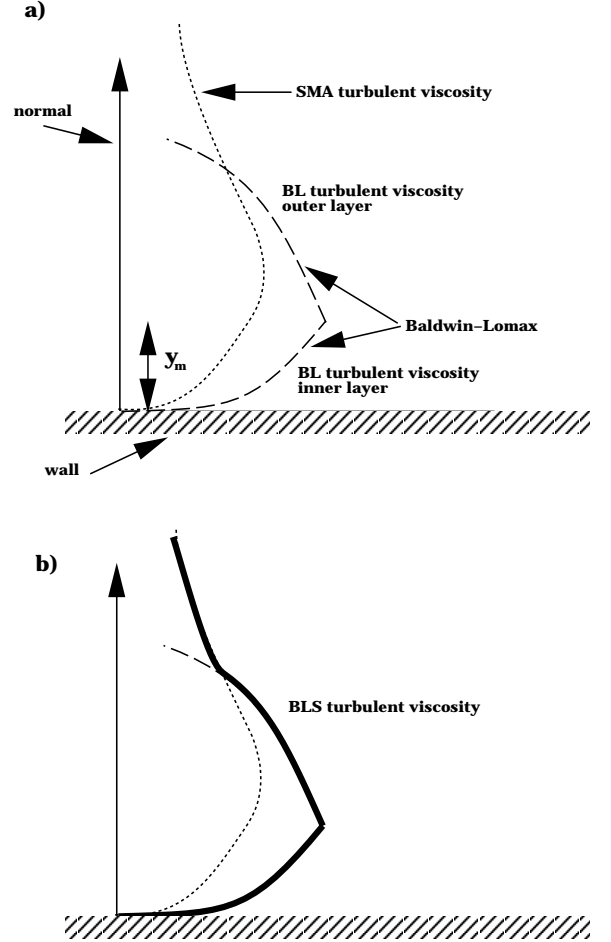


Figure 1: (a) Viscosity for Baldwin Lomax in the inner and the outer layer (dashed line) and the viscosity for Smagorinsky (dotted line). (b) Turbulent viscosity for the modified closure model (solid line).

The position y_m on the normal direction (Figure 1) is the distance from the wall for which $\nu_{tur_i}(y_m) = \nu_{tur_o}(y_m)$, i.e. the position that divides the inner from the outer layer in the BL model. The turbulent viscosity is calculated by marching from the wall in the normal direction until the normal ends. For the inner layer, ν_{tur_i} is calculated using BL. For the the outer layer, ν_{tur_o} is a blend of BL and SMA. The algorithm has been summarized in Table 1.

1. Calculate ν_{smag} at the points
2. Interpolate ν_{smag} from the points to the normals
3. Calculate y_{max} for Baldwin Lomax
4. for $y < y_{max}$
 - Calculate $\nu_{turb} = \nu_{bl}$ at normal point
5. for $y > y_{max}$ until normal ends
 - Calculate $\nu_{turb} = \nu_{bl}$ until $\nu_{bl} = \nu_{smag}$
 - Then $\nu_{turb} = \nu_{smag}$
6. Interpolate from normals to points

Table 1: BLS Algorithm

We note that a similar approach is mentioned by Mason [3], who points out the lack of accuracy of LES near walls and proposes the calculation of the viscosity near the wall as

$$\nu_t = \kappa(y + y_0)^2 \frac{\partial U}{\partial y}. \quad (13)$$

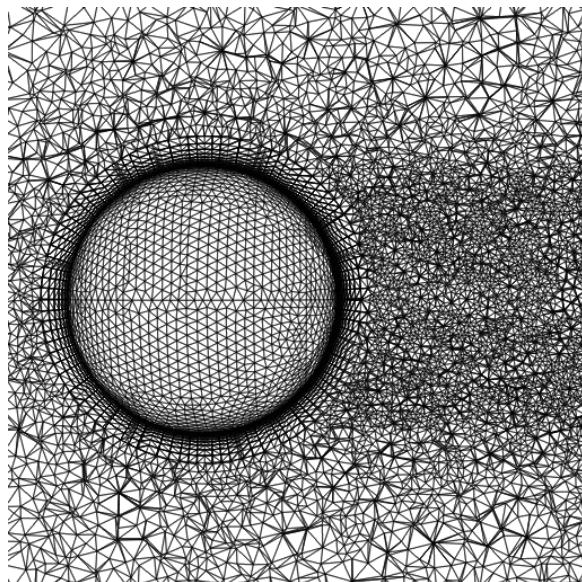
and in the core flow maintains the traditional Smagorinsky closure, matching both viscosities. He also mentions the possibility of exploring other functions, for example the Van Driest function (Equation (3)). This new model does not represent any extra work in the implementation because it requires the same quantities calculated in BL and Smagorinsky models.

Results

Three different cases were tested using the proposed model. First, a comparison for the three models is completed for the case of the flow past a sphere. Second, the BLS model is applied to the flow past a cylinder. And third, the case of the cube in a channel.

Flow past a sphere at $Re = 6 \times 10^5$

The modified method was applied to the flow past a sphere at high Reynolds number ($Re = 6 \times 10^5$). The RANS mesh for the case is shown in Figure 2. The finite element grid contains approximately 1.4M elements and 240K points.

**Figure 2:** Unstructured surface mesh for a sphere.

The same case was computed using the BLS, BL and Smagorinsky models. The drag force history for the BLS case is shown in Figure 3. The average drag coefficients obtained for the three models are compared with the experimental data [15, 16, 17, 18] in Table 2.

The drag coefficient obtained for BL and BLS overestimates the experimental C_D and are close to each other, less than 8% difference. The C_D from the Smagorinsky model is by far the worst, proving the lack of reliability to describe the flow near the wall. The calculation of the drag is affected mostly by the flow near the wall and the proper capture of the separation region. The near wall flow and separation region are well represented in the Baldwin-Lomax-Smagorinsky model.

Drag Coefficient	
$C_{D_{exp}}$	0.1
$C_{D_{BL}}$	0.156
$C_{D_{BLS}}$	0.144
$C_{D_{SMAG}}$	0.506

Table 2: Drag Coefficients for Sphere ($Re = 6 \times 10^5$)

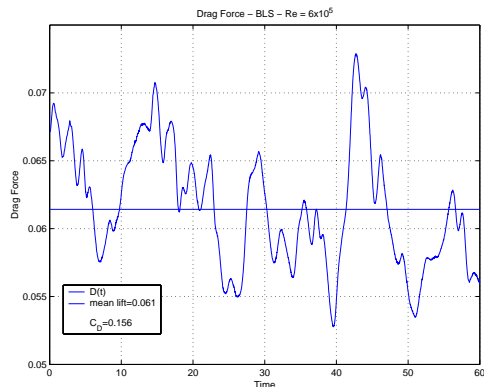


Figure 3: History drag force: BLS (solid line).

The flow structure in the wake of the sphere is depicted in Figures 4, 5 and 6. We remark that the wake is highly transient, and therefore these figures only represent a snapshot. The absolute velocity range for the three models is similar (0.0 m/s - 1.5 m/s), however the shape of the wake has some important differences. The BL and BLS share the same structure near the wall because in that region they are basically the same and the main difference comes in the inner region where the BL predicts zero turbulent viscosity and Smagorinsky does not. The Smagorinsky model has the main difference with the other two models near the wall where high velocities can be seen near the wall and the separation point is not well predicted (Figure 6). Lower velocities are in the wake for the BLS and BL models and they predict well the separation point in Figures 4 and 5 (separation at $\phi = 110^\circ$ [17]).

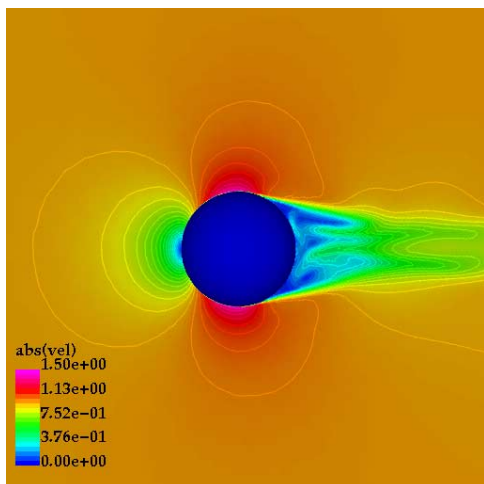


Figure 4: Absolute velocity - BLS.

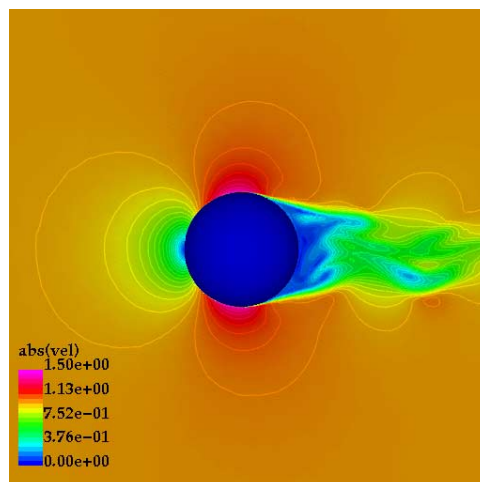


Figure 5: Absolute velocity - BL.

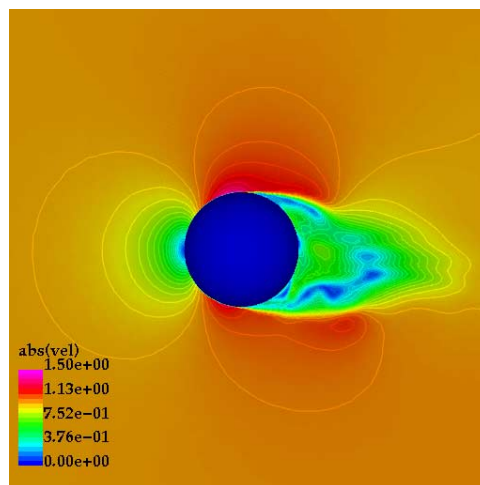


Figure 6: Absolute velocity - SMAG.

A zoom into the velocity field is shown in Figures 7, 8 and 9. The recirculation structures near the wall are similar for the BLS and BL model while the Smagorinsky model does not have the detachment region in the right position. The upwind region is similar in the three models.

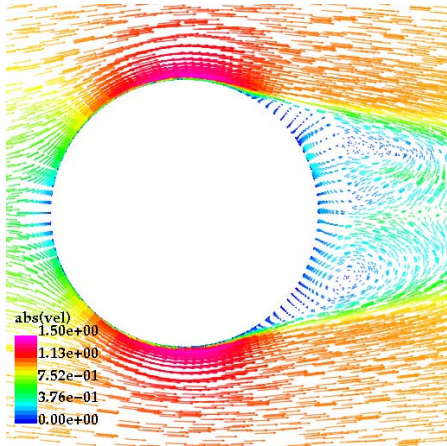


Figure 7: Velocity field - BLS.

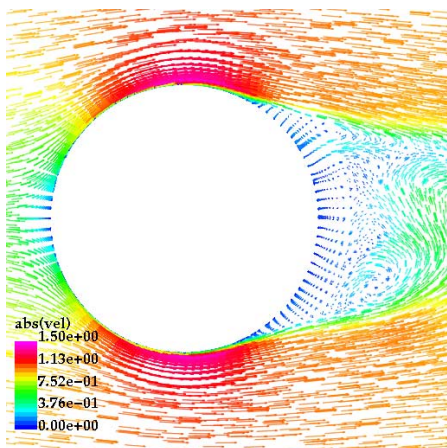


Figure 8: Velocity field - BL.

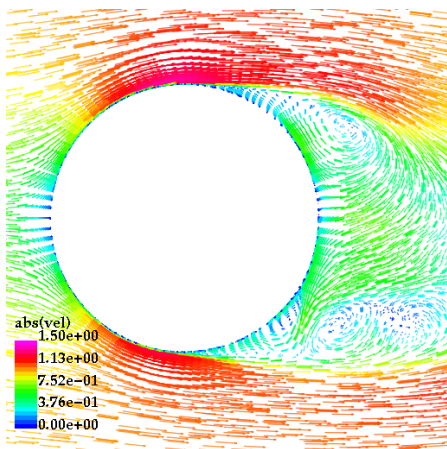


Figure 9: Velocity field - SMAG.

Pressure shadings over the sphere and in a cut plane are shown in Figures 10, 11 and 12. The BLS and BL are very similar again while the Smagorinsky model presents a substantial difference with the other models. Such difference is due to the bad representation of the physics near the wall by the model.

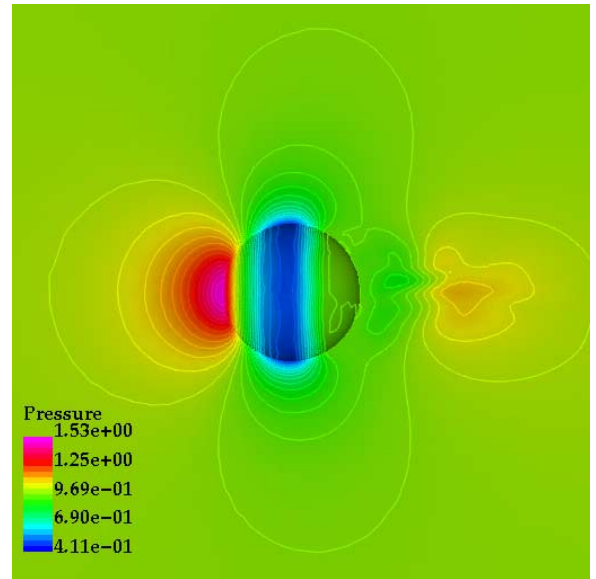


Figure 10: Pressure - BLS.

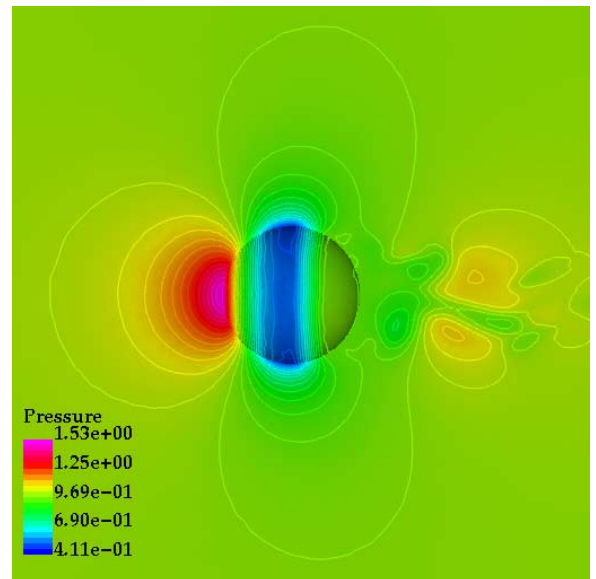


Figure 11: Pressure - BL.

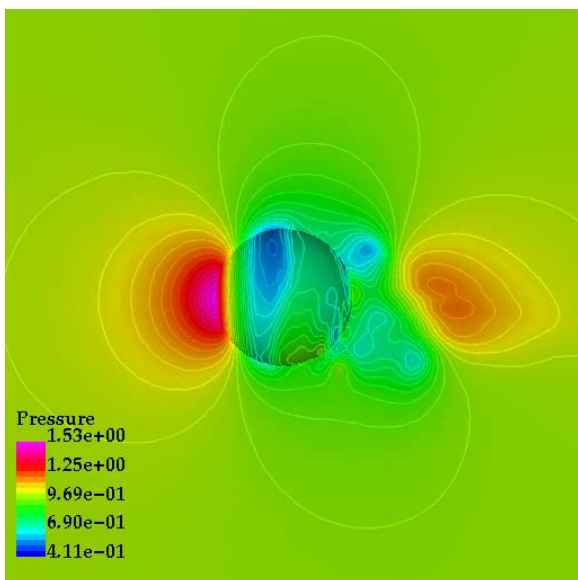


Figure 12: Pressure - SMAG.

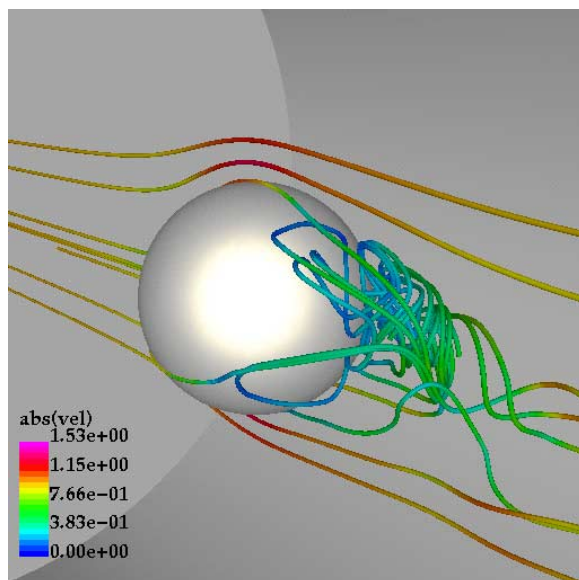


Figure 14: Ribbons - BLS.

The iso-surface of zero velocity in the component of the main flow direction (x axis) is calculated to capture the separation region behind the sphere (Figure 13).

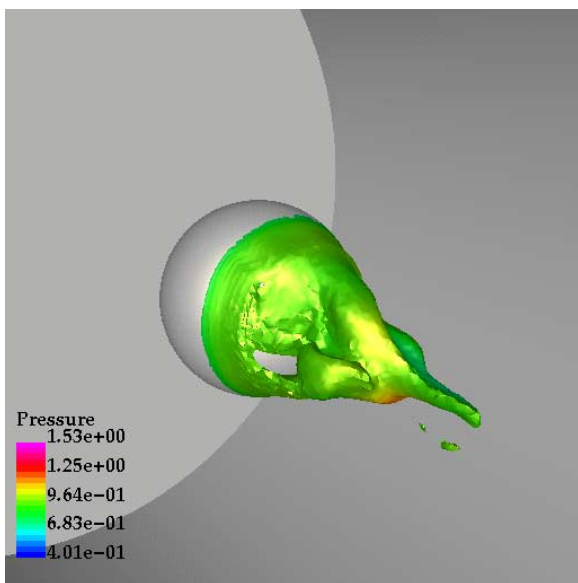


Figure 13: Iso-surface of $u = 0$ - BLS.

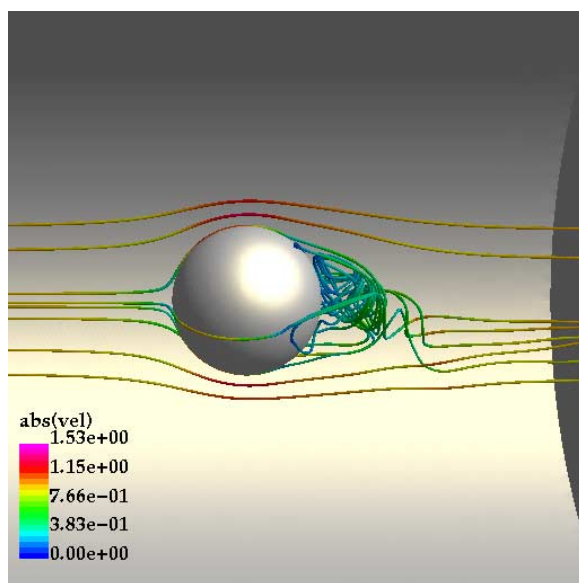


Figure 15: Ribbons - BLS.

The complex flow pattern in the wake of the sphere is illustrated with ribbons colored with the absolute value of the velocity in Figures 14 and 15.

We can conclude that the proposed model represents properly the patterns of the flow past a sphere at high Reynolds number. However, there is little improvement of the calculation on the C_D coefficient for the new model when compared to the traditional BL model. The new model represents an easy approach to DES and can be applied to either truly transient problems (where a RANS model does not work) or wall dominated problems (where Smagorinsky does not work).

Flow past a cylinder at $Re = 4 \times 10^6$

The BLS model was used to simulate the flow past a cylinder at $Re = 4 \times 10^6$. The finite element grid for the cylinder case contains approximately 500K elements and 93K points. The surface mesh is shown in Figure 16. The Strouhal number obtained from the simulation is $S = 0.276$ (Figure 17). When the Strouhal number is compared with the experimental the difference is less than 10% ($S = 0.256$ [17]).

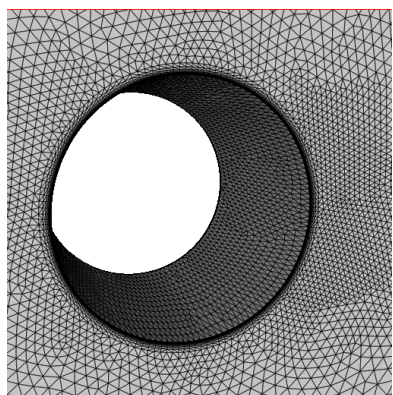


Figure 16: Unstructured surface mesh for a cylinder.

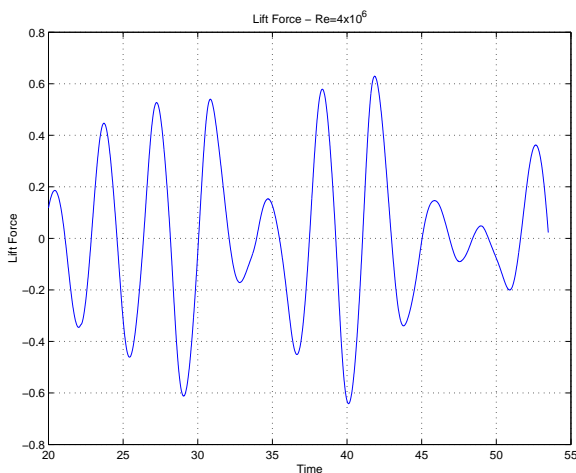


Figure 17: Lift force vs time.

The time history for lift force in Figure 17 presents a similar period between peaks but the amplitude is changing without a pattern, a characteristic of turbulent flows. Two snapshots for pressure and velocity are shown in Figures 18, 19, 20 and 21. Packets of low pressure are detaching from the back of the cylinder forming a von Kármán pattern in the wake. Those low pressure regions

are captured in two different times to show the mainly nonuniform behavior for the flow in this turbulent situation. The vector plots in Figures 20 and 21 show the displacement of the separation point with time.

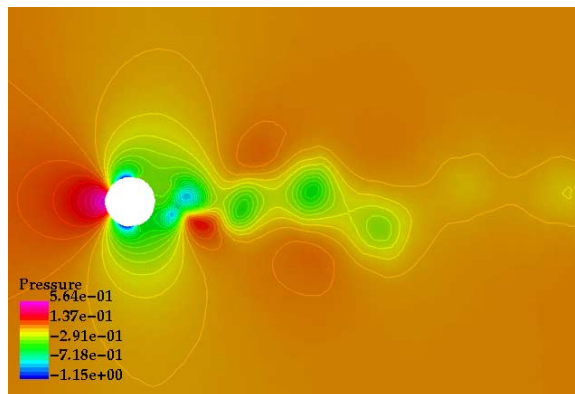


Figure 18: Pressure - BLS - Time = 20.

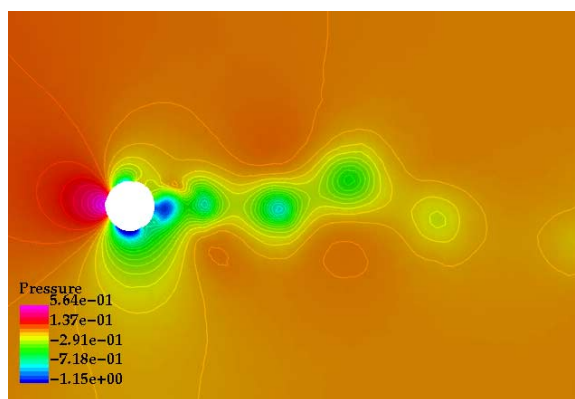


Figure 19: Pressure - BLS - Time = 40.

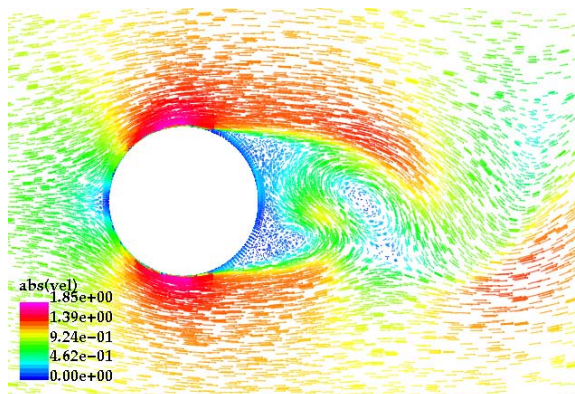


Figure 20: Velocity field - BLS - Time = 20.

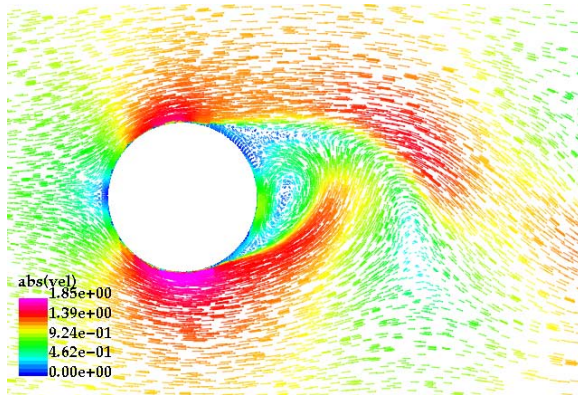


Figure 21: Velocity field - BLS - Time = 40.

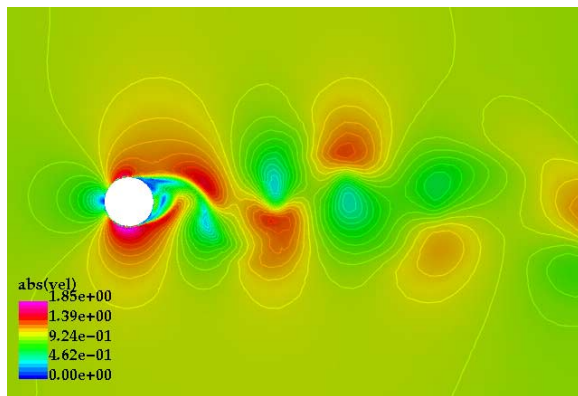


Figure 22: Absolute velocity - BLS - Time = 40.

Figure 22 shows the Kármán vortex street for a particular time. Figures 23 and 24 show ribbons for the cylinder. Figure 23 zooms in the back of the cylinder showing the complexity of the flow structure close to the wall, while Figure 24 zooms out showing the variation in the flow direction in the wake.

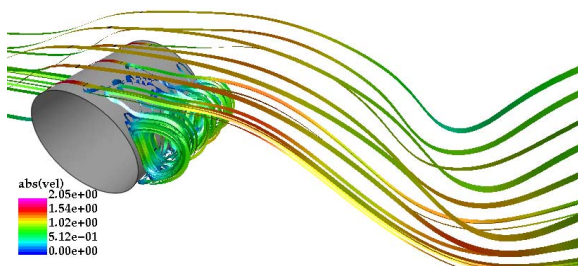


Figure 23: Ribbons - BLS.

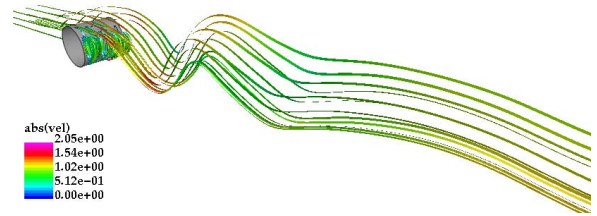


Figure 24: Ribbons - BLS.

Cube in a channel at $Re = 4 \times 10^5$

The flow around bluff bodies has been studied many times in the past decades [19, 20, 21, 22]. The importance of capturing the right flow pattern around buildings at high Reynolds numbers is vital for predicting concentration levels of pollutants or poisonous gases. The new model was used to simulate a cube in a channel at $Re = 4 \times 10^5$ [23]. The initial and boundary conditions are taken from [23]. The finite element grid contains approximately 2M elements and 360K points. The surface mesh is shown in Figure 24.

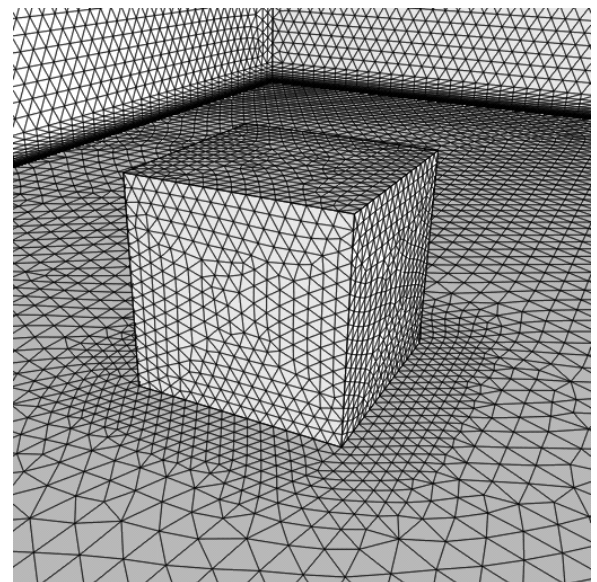


Figure 24: Unstructured surface mesh for a cube.

Mean velocity profiles were calculated (Figures 26-31) at selected positions (Figure 25) and compared with the wind tunnel profiles [24, 23].

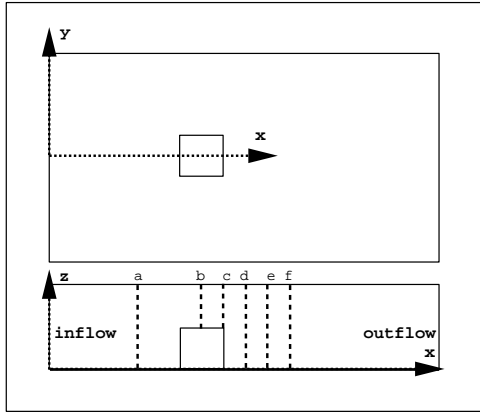


Figure 25: Geometry.

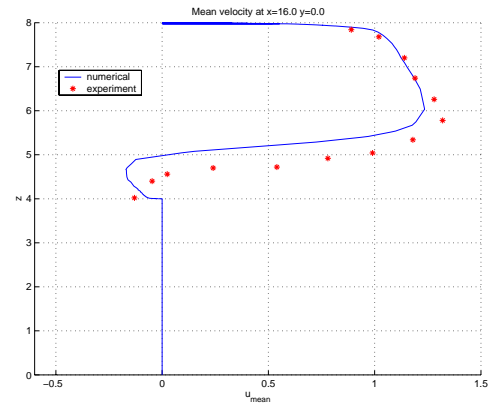


Figure 28: Mean velocity at $x=16.0$ $y=0.0$ (c).

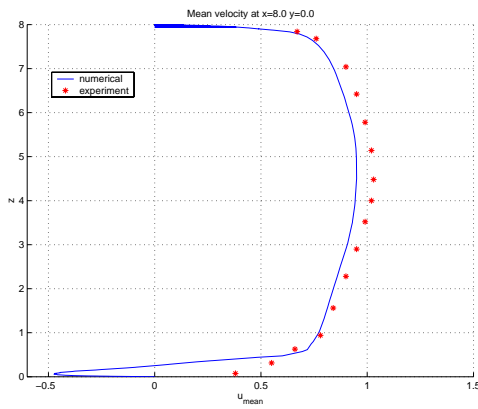


Figure 26: Mean velocity at $x=8.0$ $y=0.0$ (a).

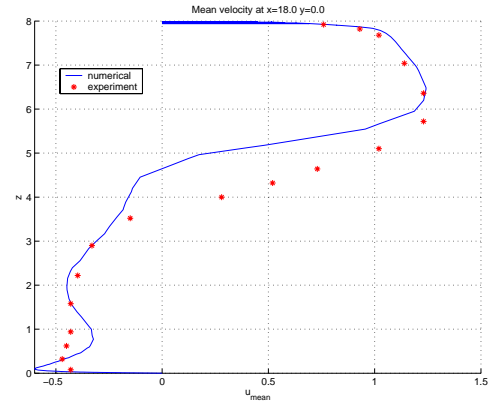


Figure 29: Mean velocity at $x=18.0$ $y=0.0$ (d).

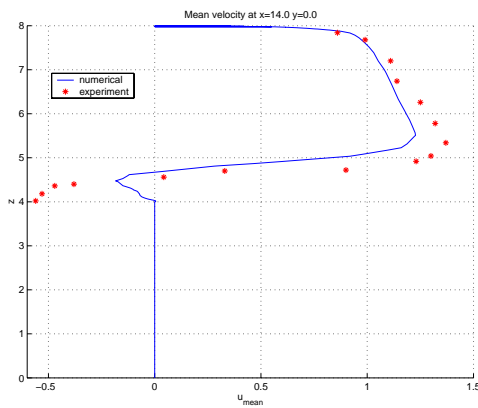


Figure 27: Mean velocity at $x=14.0$ $y=0.0$ (b).

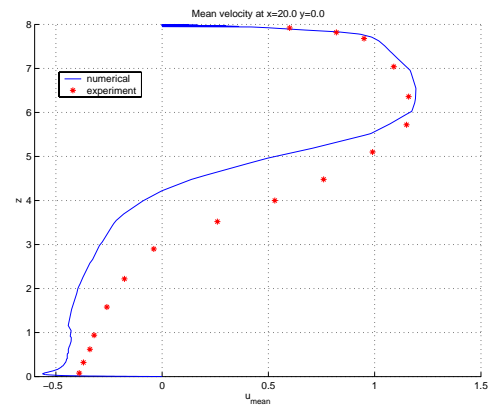


Figure 30: Mean velocity at $x=20.0$ $y=0.0$ (e).

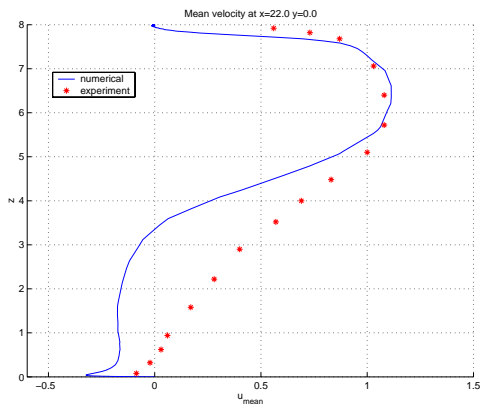


Figure 31: Mean velocity at $x=22.0$ $y=0.0$ (f).

The numerical results obtained using the BLS model agree fairly well with the experimental data obtained from [24, 23]. The BLS model proved to be an inexpensive and a suitable tool to predict the proper wind profiles in different positions (Figures 25-31).

Conclusions

A new turbulence model, based on a blend of the simplest algebraic models: Baldwin-Lomax and Smagorinsky, has been proposed. The new model, named BLS, attempts to use each one of these models where it performs best. Results for a sphere show that the new turbulence closure improves the prediction of drag considerably compared with the Smagorinsky model and gives similar results than the BL model. In the case of the cylinder at high Reynolds number the results of the new model are remarkably good, it predicts the turbulent Strouhal number with less than 10% from the one obtained experimentally. Finally, the model was applied to a cube in a channel and several mean wind profiles were computed and compared with the profiles obtained from the wind tunnel experiment. The numerical results are close to the experiments.

Summarizing, the method proposed was compared with three different situations and the results were satisfactory in each of the cases. Separation regions are well represented and experimental results match fairly well with the numerical results. The method is a good approach to blend formulations like LES and RANS in what the literature calls DES [11, 12]. The extra programming effort for codes with any Smagorinsky model and BL model are minimal. Since the wall region is resolved in a RANS sense, stretched (anisotropic) grids are required to

resolve the boundary layer. Then, the number of points is small as compared to truly LES grids. However, that can also be a disadvantage for the proposed model when it is applied to very complex geometries. The method can be extended to other kinds of flows where the presence of walls dominates the turbulence process. Other models than Smagorinsky can be used in the core flow too.

Acknowledgments

This work was partially supported by DSWA through the CHARM project at the School of Computational Sciences, George Mason University.

References

- [1] D. C. Wilcox, "Turbulence Modeling for CFD", Second Ed., *DCW Industries, Inc.*, 1998.
- [2] D. C. Wilcox, "Turbulence Modeling: An Overview" *AIAA Paper 2001-0724*, 2001.
- [3] P. J. Mason, "Large-Eddy Simulation: A Critical Review of the Technique", *J. R. Meteorol. Soc.*, vol. **120**, pp. 1-16, 1994.
- [4] J. Smagorinsky, "General Circulation Experiments with the Primitive Equations. I. The Basic Experiment", *Mon. Weather Rev.*, vol. **91**, pp. 99-164, 1963.
- [5] D.K. Lilly, "The Representation of Small Scale Turbulence in Numerical Simulation Experiments", *Proc. 10th IBM Scientific Comp. Symp. Env. Sc.*, T.J. Watson Research Center, Yorktown Heights pp. 195-210, 1967.
- [6] C. Fureby, and F. F. Grinstein, "Monotonically Integrated Large Eddy Simulation of Free Shear Flows", *AIAA Journal*, vol. **37**, part 5, pp. 544-556, 2001.
- [7] C. Fureby, and F. F. Grinstein, "Large Eddy Simulation of High Reynolds-Number Free and Wall-Bounded Flows", *AIAA Paper 2000-2307*, 2000.
- [8] P. Moin, and K. Mahesh, "Direct Numerical Simulation - A Tool in Turbulence Research", *Annual Review of Fluid Mech.*, vol. **30**, pp. 539-578, 1998.
- [9] N. V. Nikitin, F. Nicoud, B. Wasistho, K. D. Squires, P. R. Spalart, "An Approach to Wall Modeling in Large-Eddy Simulations", *Phys. Fluids*, vol. **12**, part 7, pp. 1629-1632, 2000.

- [10] U. Piomelli, J. Ferziger, and P. Moin, “New Approximate Boundary Conditions for Large Eddy Simulations of Wall-Bounded Flows”, *Phys. Fluids A*, vol. **1**, part 6, pp. 1061-1068, 1989.
- [11] P. R. Spalart, W. H. Jou, M. Strelets, and S. R. Allmaras, “Comments on the Feasibility of LES for Wings, and on a Hybrid RANS/LES Approach”, *First AFOSR International Conference on DNS/LES*, Rouston, Louisiana, USA, 1997.
- [12] G. S. Constantinescu, and K. D. Squires, “LES and DES Investigations of Turbulent Flow over a Sphere”, *AIAA Paper 2000-0540*, 2000.
- [13] B. S. Baldwin, and H. Lomax, “Thin-Layer Approximation and Algebraic Model for Separated Turbulent Flows”, *AIAA Paper 78-257*, 1978.
- [14] G. K. Batchelor, “An introduction to fluid dynamics”, reprinted paperback edition, *Cambridge: University Press*, 1998.
- [15] E. Achenbach, “Experiments on Flow Past Spheres at Very High Reynolds Numbers”, *J. Fluid Mech.*, vol. **54**, part 3, pp. 565-575.
- [16] S. Taneda, “Visual Observations of Flow Past a Sphere at Reynolds Numbers between 10^4 and 10^6 ”, *J. Fluid Mech.*, vol. **85**, part 1, pp. 187-192, 1978.
- [17] H. Schlichting, “Boundary-Layer Theory”, Seventh Ed., *McGraw-Hill, New York, NY*, 1979.
- [18] T. A. Johnson, and V. C. Patel, “Flow Past a Sphere up to a Reynolds Number of 300”, *J. Fluid Mech.*, vol. **378**, pp. 19-70, 1999.
- [19] I. P. Castro, and A. G. Robins, “The Flow Around Surface-Mounted Cube in Uniform and Turbulent Stream”, *J. Fluid Mech.*, vol. **79**, pp. 307-335, 1977.
- [20] R.P. Hosker, “Flow and Diffusion Near Obstacles”, in: D.Raderson (Ed.), *Atmospheric Science and Power Production. US Dept of Energy, DOE/CR-2521* (US Nuclear Regulatory Commission) (1980).
- [21] *Evaluation of Modelling Uncertainty, CFD Modelling of Near-Field Atmospheric Dispersion*. Project EMU final report (1997).
- [22] I. R. Cowan, I. P. Castro, and A. G. Robins, “Numerical Considerations for Simulations of Flow and Dispersion Around Buildings”, *J. Wind Eng. Ind. Aerodyn.*, vol. **67**, pp. 535-545, 1997.
- [23] S. Krajnović, and L. Davidson, “Large Eddy Simulation of the Flow Around a Three-Dimensional Bluff Body”, *AIAA Paper 2001-0432*, 2001.
- [24] R. Martinuzzi, and C. Tropea, “The Flow Around Surface-Mounted Prismatic Obstacles Placed in a Fully Developed Channel Flow”, *ASME: J. Fluid Mech.*, vol. **115**, pp. 85-91, 1993.